NETWORKS AND HETEROGENEOUS MEDIA
©American Institute of Mathematical Sciences
Volume **4**, Number **1**, March **2009**
doi:10.3934/nhm.2009.4.1
pp. **1–18**

SELF–MOTION OF CAMPHOR DISCS. MODEL AND ANALYSIS

Xinfu Chen

Department of Mathematics, University of Pittsburgh
Pittsburgh, PA 15260, USA

Shin-Ichiro Ei

Faculty of Mathematics, Kyushu University
Fukuoka, 812-8581, Japan

Masayasu Mimura

Meiji Institute for Advanced Study of Mathematical Sciences, Meiji University
Kawasaki, 214-8571, Japan

(Communicated by Roberto Natalini)

Abstract. In the present paper, a model describing the self-motion of a camphor disc on water is proposed. The stability of a standing camphor disc is investigated by analyzing the model equation, and a pitchfork type bifurcation diagram of a traveling spot is shown. Multiple camphor discs are also treated by the model equations, and the repulsive interaction of spots is discussed.

1. **Introduction.** In order to clarify biological and molecular motors, autonomous motors under isothermal conditions have been investigated experimentally and through mathematical modeling. For example, the driving force behind the self-motion of a floating camphor scraping has been explained as being due to the difference in the surface tension around the camphor scraping ([3], for instance). However, this explanation raises a number of questions. Will the camphor move under small asymmetric disturbances if the camphor is disc shaped? If the disc does move in a rectangular water vessel, what is the motion of the disc? In order to investigate these questions experimentally, we prepare a water phase in a square polystyrene cell (length: 200 mm; depth: 50 mm) and drop a camphor disc (diameter: 13.5 mm, thickness: 0.5 mm, weight: 0.1 g, pure camphor) onto the water phase. Figure 1 shows the trajectory of a disc that moves continuously for 10 seconds. The camphor disc was observed to move. In addition, when the disc approaches a wall, it changes direction before colliding with the wall, as if it were an elastic body.

2000 *Mathematics Subject Classification.* Primary: 80A30, 58J55, 35K55, 35K57; Secondary: 93A30.

Key words and phrases. camphor discs, repulsive interaction, center manifold theory, traveling spot.

Authors thank referees for their valuable comments and suggestions. The first author is supported in part by a grant from the National Science Foundation (DMS-9971043,0203991, and 0504691) and the second and third authors are supported in part by Grants-in-Aid for Scientific Research ((C) No.16540200 and (S) No.18104002), respectively, from JSPS.

The goal of the present paper is to understand these phenomena by using a mathematical model. In Section 2, we introduce a mathematical model to describe the motion of several camphor discs floating on the water phase. In Section 3, we consider a single disc in the space $\mathbb{R}^2$ and discuss the existence and stability of a radially symmetric equilibrium solution corresponding to a motionless disc. It is shown that, in some parameter range, the disc loses its stability. This destabilization implies that the camphor disc moves under small non-radially symmetric disturbances. In Section 4, we consider the interaction of camphor discs.

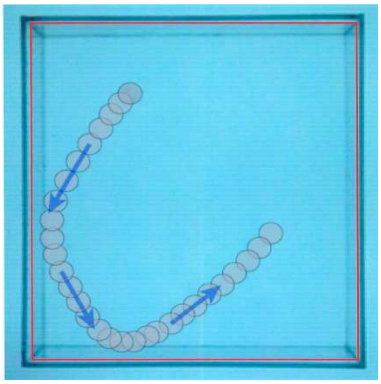

FIGURE 1. A camphor disc moving in a square vessel of water phase.

2. **Mathematical modeling.**

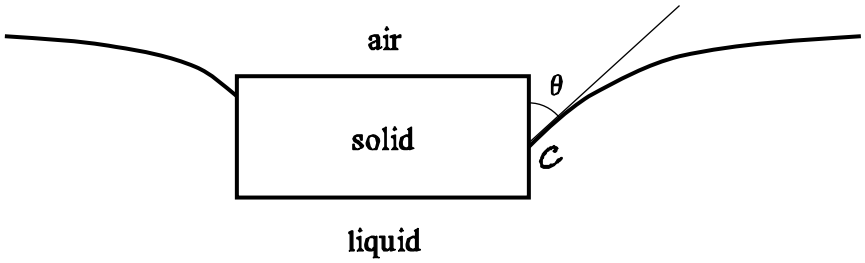

FIGURE 2. A cross section view of the camphor disc in water.

2.1. **Driving force for the motion of a camphor disc.** We believe that the driving force behind the motion of a camphor disc is the surface tension. Surface tension is caused by the attraction between the liquid's molecules by various intermolecular forces. In the bulk of the liquid, each molecule is pulled equally in all directions by neighboring liquid molecules, resulting in a net force of zero. At the liquid-solid and liquid-air interfaces, the molecules are pulled inwards by other molecules deeper inside the liquid and are not attracted as intensely by the molecules in the neighboring medium. Therefore, all of the molecules at the surface are subject to an inward force of molecular attraction which is balanced only by the liquid's resistance to compression, meaning there is no net inward force. Mathematically, surface tension, represented by the symbol σ, is defined as the force along a

line of unit length, where the force is parallel to the surface but perpendicular to the line. It has the unit of dyn/cm.

We denote by $\sigma_{ls}, \sigma_{la}, \sigma_{as}$ the surface tension of liquid-solid, liquid-air, and solid-air, respectively. We assume that σ_{ls} and σ_{as} depend on the (surface) concentration of camphor that is dissolved in the water. Using $x = (x_1, x_2)$ for plane coordinates and t for time, we denote by $c = c(x,t)$ (mol/cm^2) the surface concentration of camphor in liquid. Thus, the surface tension σ_{ls} and σ_{la} is a function of c.

Denote by r the radius of the camphor disc and by $p = p(t)$ the center of disc at time t. The location of the disc is then at $B(p,r) := \{x \in \mathbb{R}^2 \mid |x-p| < r\}$. The boundary of the disc is denoted by $\partial B(p,r)$.

We divide the total contribution of surface tension into three pieces.

(1) In Figure 2, we denote by $\mathcal{C}$ the tri-intersection of the air-liquid-solid which can be regarded as a circle. Take from $\mathcal{C}$ a piece of length ds, with horizontal projected unit normal $\vec{n}$. The net driving force in the horizontal direction is

$$d\vec{f_1} = \vec{n}\ ds\ \sigma_{la}\ \sin\theta,$$

where θ (also a function of c) is the contact angel determined by the balance of surface tension in the vertical direction

$$\sigma_{ls} - \sigma_{sa} = -\sigma_{la}\cos\theta.$$

Eliminating θ we obtain

$$d\vec{f_1} = \vec{n}\ ds\ \sigma_{la}\sqrt{1-(\sigma_{ls}-\sigma_{sa})^2/\sigma_{la}^2}.$$

The total contribution of the surface tension along the tri-intersection $\mathcal{C}$ is

$$\vec{f_1} = \int_{\partial B(p,r)} \sqrt{1-(\sigma_{ls}-\sigma_{sa})^2/\sigma_{la}^2}\ \sigma_{la}\ \vec{n}\ ds.$$

(2) Since surface tension is in the direction tangential to the surface, there is no horizontal force contributed by the lateral surface of the disc.

(3) On the bottom surface of the camphor disc, the surface tension is not uniform since σ_{ls} depends on the concentration. The surface tension differences cause a well-known Marangoni effect (sometimes also called the Gibbs-Marangoni effect). Since a liquid with a high surface tension pulls more strongly on the surrounding liquid than one with a low surface tension, the presence of a gradient in surface tension will naturally cause the liquid to flow away from regions of low surface tension. Regarding the motion of liquid as driving force given towards the camphor disc, the total contribution can be calculated as

$$\vec{f_3} = \int_{B(p,r)} \nabla\sigma_{ls}\ dx = \int_{\partial B(p,r)} \sigma_{ls}\ \vec{n}\ ds.$$

Here in the second equation, we have used the divergence theorem.

We see that the total surface tension can be written as

$$\vec{F}_{ST} = \vec{f_1} + \vec{0} + \vec{f_3} = \int_{\partial B(p,r)} \Gamma\ d\vec{s},$$

where

$$d\vec{s} = \vec{n}\,ds, \quad \Gamma = \sigma_{ls} + \sigma_{la}\sqrt{1-(\sigma_{ls}-\sigma_{sa})^2/\sigma_{la}^2}.$$

We assume that $\Gamma = \Gamma(c)$ depends only on the surface camphor concentration c.

Laboratory experiments suggest that

$$\Gamma(c) = \frac{\Gamma_0}{1 + Ac},$$

where A is approximately a positive constant (which may depend on temperature [3]). In general, if $c = 1$ represents saturation, then $\Gamma(0)/\Gamma(1) = 1 + A$ can be significantly large. That is to say, the forces on various parts of the disc may be very unbalanced if the concentration at different points on the disc surface are very different.

Although only a small amount of camphor is dissolved into the water tank, and consequently the mean concentration (or the concentration a few millimeters away from the disk) can be considered to be zero, the concentration near the camphor surface can be very high. When a camphor disc is in motion, the concentration difference at the lateral boundary of the disc can be significant. The front edge of the disc continues to move toward areas of fresh water in which the concentration is low and the molecular pulling force is large, whereas the back edge of the disc moves into areas of previous dissolution, in which the concentration is high and the molecular dragging force is small. We believe that this net difference in the pulling and dragging forces is the mechanism that causes a camphor disc to move with a constant velocity, as was observed in a laboratory experiment.

As mentioned, the Marangoni effect will cause the motion of liquid, so does the motion of camphor disc. Since the motion of camphor disc is not very large, at this stage, we shall not take into account the motion of liquid.

2.2. **Equation of motion for a single camphor disc.** Due to the above-described driving force, the camphor disc will move if not secured. When the disc is in motion, the liquid will apply a viscous force on the disc. Since the disc is thin, the forces on the edge can be neglected. Hence, we can assume that the viscous motion resisting force is in the negative direction of motion and is proportional to the speed and the area of contact. Thus, the viscous force can be written as

$$\int_{\partial B(P,r)} \vec{F}_{\text{vis}} d\vec{s} = -\mu\pi r^2 \dot{P}(t),$$

where μ (dyn$\cdot$ sec/cm^2) is the viscous coefficient, and $P(t)$ is the center of the disc. The motion equation for the solid camphor disc can then be written as

$$(\rho_c \pi r^2 h)\ddot{P}(t) = \vec{F}_{\text{ST}} + \int_{\partial B(P,r)} \vec{F}_{\text{vis}} d\vec{s} = \int_{\partial B(P,r)} \Gamma(c)\, d\vec{s} - \mu\pi r^2 \dot{P},$$

where ρ_c is the density of the camphor disc, and h is the thickness. Since h is small and the motion of the camphor disc is observed to have an almost-constant-velocity motion, the acceleration term $\rho\pi r^2 \hat{h}\ddot{P}$ on the left-hand side can be neglected. Therefore, we can obtain the approximate equation of motion for the camphor disc, as follows:

$$\dot{P} = \frac{1}{\mu\pi r^2} \int_{\partial B(P,r)} \Gamma(c) d\vec{s}. \tag{1}$$

In the time interval of interest, for simplicity, we shall assume that the size of the camphor does not change, i.e., we assume hereafter $h = h_0$ and $r = r_0$ for constants h_0, $r_0 > 0$.

2.3. **Diffusion of the camphor in its solution.** As mentioned earlier, the large size of the water tank (compared to the camphor disc) makes the mean concentration of camphor approximately zero. Nevertheless, the concentration near the surface of the camphor disc can be very high, and so the gradient of the contraction may not be small.

Since camphor does not dilute into water very well, we only consider diffusion of camphor on the surface. Hence, we use $c(x_1, x_2, t)$ (mol/cm^2) to denote the surface concentration of camphor.

We assume that there are a total of three effects that cause the change of surface concentration of camphor in liquid. The first is the classical diffusion for which we introduce a constant, D (cm^2/sec), for the diffusion coefficient of camphor in water. Since camphor evaporates, we use $-\alpha c$ to denote the decreasing rate of change of concentration due to evaporation, where α can be a (small) constant or a function of c. Finally, we use $\tilde{F}(c)$ to denote the rate of dissolution of camphor from disc to water, which should be a decreasing function from the phenomenological point of view. Combining these three effect, we end with the reaction-diffusion equation

$$c_t = D\Delta c - \alpha\, c\, \chi_{\Omega\setminus B(P,r_0)} + \tilde{F}(c)\chi_{B(P,r_0)}, \quad (x,t) \in \Omega \times (0,\infty),$$

where χ_A is the characteristic function of the set A. Set $F(c) = \tilde{F}(c) + \alpha c$, the above equation can be written as

$$c_t = D\Delta c - \alpha\, c\, + F(c)\chi_{B(P,r_0)}, \quad (x,t) \in \Omega \times (0,\infty). \tag{2}$$

2.4. **A moving boundary model for interaction of camphor discs.** We can now formulate the self-motion of camphor discs as follows. Assume that there are m disks, of radius $r_1, \cdots, r_m$, respectively. We search for functions $c(x,t)$ and $P_1(t), \cdots, P_m(t)$, such that

$$\begin{cases} c_t = D\Delta c - \alpha\, c + F(c)\sum_{j=1}^m \chi_{B(P_j,r_j)}(x), & x \in \Omega,\ t \in (0,\infty), \\ \dot{P}_j(t) = \beta_j \int_{\partial B(P_j,r_j)} \Gamma(c) d\vec{s}, & t > 0,\ j = 1, \cdots, m, \\ \partial_n c = 0, & x \in \partial\Omega,\ t > 0, \end{cases} \tag{3}$$

where β_j is given by

$$\beta_j = \frac{1}{\pi\mu r_j^2}.$$

Clearly, the parameters μ, α and the structural functions Γ and F depend on environmental factors, such as the temperature.

With appropriate initial conditions $(c(\cdot,0), P_1(0), \cdots, P_m(0))$, the system (3) is well-posed and has a unique global solution.

In the following sections, we show that when $m = 1$ and $\Omega = \mathbb{R}^2$, (3) has a radially symmetric solution with $P_1(t) \equiv (0,0)$ for all $t > 0$ and that in a certain parameter range, this solution is unstable and generates a bifurcating traveling spot having constant velocity. Finally, we shall discuss the interactions between different camphor discs.

3. **A single camphor disc in $\mathbb{R}^2$.** In this section, we consider a single camphor disc (i.e. $m = 1$) and hereinafter assume that $\Omega = \mathbb{R}^2$. We write (P_1, r_1, β_1) simply as (P, r_0, β). Thus, we need to find $(c(x,t), P(t))$, $x \in \mathbb{R}^2, t > 0$, such that

$$\begin{cases} c_t(x,t) = D\Delta c - \alpha\, c + F(c)H(r_0 - |x - P|), & x \in \Omega,\ t \in (0,\infty), \\ \dot{P}(t) = \beta \int_{C_{r_0}} \Gamma(c(P+x)) d\vec{s}, & t > 0, \end{cases} \tag{4}$$

where $C_{r_0} = \{x \in \mathbb{R}^2 | \, |x| = r_0\}$ is a circle of radius r_0 centered at the origin, and H is the Heaviside function: $H(\xi) = 0$ for $\xi < 0$ and $H(\xi) = 1$ for $\xi > 0$.

When we consider only one disc, it is convenient to change the variables via

$$y = x - P(t), \quad u(y,t) = c(P(t) + y, t). \tag{5}$$

The system (1) can then be written as a single non-local equation, for $u(y,t)$,

$$u_t = D\Delta u - \alpha u + \beta \int_{C_{r_0}} \Gamma(u) d\vec{s} \cdot \nabla u + F(u)H(r - |y|), \qquad y \in \mathbb{R}^2, t > 0. \tag{6}$$

Once we find u, the function P can be recovered by integrating

$$\dot{P} = \beta \int_{C_{r_0}} \Gamma(u) \, d\vec{s}.$$

3.1. **A radially symmetric equilibrium solution (standing spot).** By symmetry, (3) admits a radially symmetric equilibrium, given by $u(y,t) = S(|y|)$, where $S(r)$ solves

$$\begin{cases} D(S'' + r^{-1}S') - \alpha S + F(S)H(r_0 - r) = 0, & r \in (0, \infty), \\ S'(0) = 0, \quad S(\infty) = 0. \end{cases} \tag{7}$$

Note that $\dot{P} \equiv 0$ for all $t > 0$, and hence the disc does not move.

In the following, we shall analyze the stability of this steady state solution. We shall show that in some parameter range, this steady state lost its stability, and hence small perturbation from radial symmetry will give rise to the motion of a camphor disc.

3.2. **Linear stability of the standing spot.** There are two ways to linearize our problem. The first is to linearize the original system (1), which will be useful in the case of multiple discs. The second is to linearize (4), which works only for a single disc, but the calculation is simpler.

As shown later herein, the loss of stability of the equilibrium near a critical parameter is shown in different ways for the linearizations of (3) and (1), respectively.

For (3), the change in stability of the radially symmetric equilibrium is shown by the change of the sign of the principle eigenvalue of the linearized operator L *on the right-hand side of (3), the eigenspace of which is spanned by* $\{\psi(r)\cos\theta, \psi(r)\sin\theta\}$ *for some positive* ψ*, where* (r, θ) *are the polar coordinates. This eigenspace corresponds to spatial dilation.*

For (1), the linearized operator $\mathbf{L}$ *of the right-hand side of (3) always has zero as its eigenvalue with eigenspace spanned by* $\{(-S_{x_j}, \mathbf{e}_j)\}$, $j = 1, 2$*, which corresponds to the spatial dilation invariance of the system (1). The change in stability of the radially symmetric equilibrium is shown by the change in the algebraic simplicity of the eigenvalue* 0 *of* $\mathbf{L}$*, namely, a Jordan block appears.*

In the following section, we first consider the linearization of (3), and then return to (1).

3.3. **Linearization of (3).** Equation (3) can be written as

$$u_t = \mathrm{A}(u), \qquad \mathrm{A}(u) := D\Delta u - \alpha\, u + \beta \int_{C_{r_0}} \gamma(u) d\vec{s} \cdot \nabla u + F(u)H(r_0 - |y|). \tag{8}$$

Its linearization around $u(x,t) = S(|y|)$ can be written as

$$\phi_t = \mathrm{L}\phi, \tag{9}$$

where

$$\mathrm{L}\phi := \{D\Delta - \alpha + F'(S)H(r_0 - |y|)\}\phi + \beta\Gamma'(S(r))\nabla S \cdot \int_{C_{r_0}} \phi \, d\vec{s}. \tag{10}$$

The equilibrium is linearly stable, if the spectrum of L lies on the left-half complex plane; otherwise, it is unstable.

Now, we consider the eigenvalue problem

$$\mathrm{L}\phi = \lambda\phi. \tag{11}$$

This problem can be rewritten as follows: Find (λ, ϕ) and vector $\vec{v} = (v_1, v_2)$, such that

$$\begin{cases} \vec{v} = \beta\Gamma'(S(r_0)) \int_{C_{r_0}} \phi \, d\vec{s}, \\ \{-D\Delta - F'(S)H + \alpha + \lambda\}\phi = \vec{v} \cdot \nabla U. \end{cases} \tag{12}$$

Note that the vector $\vec{v}$ is related to the velocity of the motion of the disc. The velocity for the linearized system is $\dot{P} = \vec{v}e^{\lambda t}$.

In polar coordinates $y = (r\cos\theta, r\sin\theta)$, (9) can be easily analyzed.

When $\lambda \notin (-\infty, -\alpha]$, the second equation in (9) has a unique solution ϕ given by

$$\phi = \psi(r, \lambda)\Big(v_1 \cos\theta + v_2 \sin\theta\Big), \tag{13}$$

where $\psi(r, \lambda)$ is a unique solution of

$$\begin{cases} (\mathrm{L}_R^1 + \lambda)\psi = S'(r), \quad \rho > 0, \\ \psi_r(0, \lambda) = 0, \psi(\infty, \lambda) = 0, \end{cases} \tag{14}$$

$$\mathrm{L}_R^1\psi := \Big[- D\Big(\frac{d^2}{dr^2} + \frac{1}{r}\frac{d}{dr} - \frac{1}{r^2}\Big) - F'(S(r))H(r_0 - r) + \alpha\Big]\psi.$$

Hence, for $\mathrm{Re}(\lambda) > -\alpha$, (λ, ϕ) is an eigenpair if and only if the first equation in (9) holds for some non-trivial $\vec{v}$, when we substitute ϕ by (10).

For ϕ in (10), it is easy to find

$$\int_{C_{r_0}} \phi \, d\vec{s} = \pi r_0 \psi(r_0, \lambda) \, \vec{v}.$$

Hence, we have the following:

Lemma 3.1. *$\lambda \notin (-\infty, -\alpha]$ is an eigenvalue of* L *if and only if*

$$-\psi(r_0, \lambda) = b := \frac{1}{\pi r_0 \beta |\Gamma'(S(r_0))|}. \tag{15}$$

If this equation is satisfied, then the eigenspace, for ϕ, is spanned by

$$\{\psi(r, \lambda)\cos\theta, \psi(r, \lambda)\sin\theta)\}.$$

Recall that $\Gamma'(c) < 0$.

Lemma 3.2. *All of the eigenvalues of* L *are real.*

Proof. Equipped with inner product

$$(\psi_1, \psi_1)_R := 2\pi \int_0^\infty r\psi_1\overline{\psi_2} \, dr$$

the operator L_R^1 is positive definite. In addition, differentiating (4) with respect to r gives

$$\mathrm{L}_R^1 S' = -F(S(r_0))\delta_{r_0}, \tag{16}$$

where δ_{r_0} is the Dirac measure with mass at $r = r_0$.

Now, assume that $\lambda \notin (-\infty, -\alpha]$ is an eigenvalue of L. Taking the inner product of $(\mathrm{L}_R^1+\lambda)\psi = S'$ with ψ and S', respectively, and using $(\mathrm{L}_R^1\psi, S')_R = (\psi, \mathrm{L}_R^1 S')_R = -2\pi r_0 \psi(r_0, \lambda)F(S(r_0))$, we obtain

$$\lambda\|\psi\|_R^2 = (S', \psi)_R - (\mathrm{L}_R^1\psi, \psi)_R, \quad \lambda(\psi, S')_R = \|S'\|_R^2 + 2\pi r_0\psi(r_0, \lambda)F(S(r_0)). \tag{17}$$

Using $(\psi, S')_R = \overline{(S', \psi)_R}$, we then obtain

$$|\lambda|^2\|\psi\|_R^2 = \|S'\|_R^2 + 2\pi r_0\bar{\psi}(r_0, \lambda)F(S(r_0)) - \bar{\lambda}(\mathrm{L}_R^1\psi, \psi)_R.$$

Since $\psi(r_0, \lambda) = -b$ is real and $(\mathrm{L}_R^1\psi, \psi)_R$ is positive, λ must be real. □

Lemma 3.3. *Let $\sigma(\mathrm{L})$ be the spectrum of* L. *Then,*

$$\sigma(\mathrm{L}) = (-\infty, -\alpha] \cup \{\lambda^*(b)\}$$

where $\lambda^*(b)$, the solution to (12), is real and satisfies the following: Define

$$b^* := \frac{\|S'\|_R^2}{2\pi r_0 F(S(r_0))}.$$

Therefore, $\lambda(b^*) = 0$, $\frac{d}{db}\lambda^*(b^*) < 0$ and $\lambda^*(b) < 0$ if and only if $b > b^*$.

Proof. From the equation $\mathrm{L}_R^1 S' = -F(S(r_0))\delta_{r_0}$ we see that $S' < 0$ for all $r \in (0, \infty)$. Consequently, for real $\lambda > -\alpha$, $\psi(r, \lambda) = (\mathrm{L}_R^1 + \lambda)^{-1}S' < 0$ for all $r \geq 0$, $|\psi(r_0, \lambda)|$ is a decreasing function of λ, and $\lim_{\lambda\to\infty} |\psi(r_0, \lambda)| = 0$. Hence, for every $b > 0$, (12) has a unique solution $\lambda = \lambda^*(b)$ (When $b > |\psi(r_0, -\alpha)|$, we simply define $\lambda^*(b) = -\alpha$). From (14), we see that when $\lambda = 0$, $\psi(r, 0) = -b^*$. It follows that $\lambda^*(b^*) = 0$, $\frac{d}{db}\lambda^*(b^*) < 0$, and $\lambda^*(b) < 0$ if and only if $b > b^*$. This completes the proof. □

Remark 1. From the above discussion, we see that the equilibrium is linearly stable if and only if $b > b^*$; that is, the radially symmetric equilibrium is linearly stable if and only if

$$\beta := \frac{1}{\pi\mu r_0^2} < \frac{2F(S(r_0))}{|\Gamma'(S(r_0))| \int_0^\infty rS'^2(r)\, dr}, \tag{18}$$

where r_0 is the radius of the disc, and S is the solution to (4).

3.4. **Linearization of (1).** To clarify the difference and relationship between the linearizations of (1) and (3) mentioned above, we investigate the linearization of (1).

Since the derivative of the Heaviside function is the Dirac mass and $\int_{C_{r_0}} (\nabla S \cdot P)\, d\vec{n} = \pi r_0 S'(r_0)P$, the linearization of (1) around the equilibrium $(S(|x|), 0)$ takes the form

$$\begin{bmatrix} \phi \\ P \end{bmatrix}_t = \mathbf{L}\begin{bmatrix} \phi \\ P \end{bmatrix} := \begin{bmatrix} (D\Delta - \alpha + F'H)\phi + F\delta_{C_{r_0}}\mathbf{e}(\theta)\cdot P \\ \beta\Gamma'(S(r_0))[\pi r_0 S'(r_0)P + \int_{C_{r_0}} \phi\, d\vec{s}] \end{bmatrix}, \tag{19}$$

where $\delta_{C_{r_0}}$ is the Dirac measure with mass on the circle C_{r_0}, namely, $\int_{\mathbb{R}^2} \delta_{C_{r_0}}\zeta(x)dx = \int_{C_{r_0}} \zeta ds$ for any continuous function ζ and $\mathbf{e}(\theta) := (\cos\theta, \sin\theta)^T$.

In the sequel, we denote $\Phi = (\phi, P)^T$, where T denotes the transpose. Next, we investigate the eigenvalue problem

$$\lambda\Phi = \mathbf{L}\Phi \tag{20}$$

It is easy to see that the continuum spectrum of $\mathbf{L}$ is $(-\infty, -\alpha]$, whereas the rests are point spectrum. Since for each $P \in \mathbb{R}^2$, $(c, P) = (S(|x-P|), P)$ is in equilibrium with (1), after differentiating with respect to P, for any $\vec{v} \in \mathbb{R}^2$, $\Phi = (-\nabla S \cdot \vec{v}, \vec{v})^T$ is an eigenfunction of $\mathbf{L}$ with eigenvalue zero. Thus, 0 is an eigenvalue of $\mathbf{L}$ with an eigenspace of at least two dimensions.

Let $P = (p_1, p_2)$. Note that in polar coordinates, $F\delta_{C_{r_0}}\mathbf{e}(\theta) \cdot P = F(S(r_0))(p_1\cos\theta + p_2\sin\theta)\delta_{r_0}$. Hence, as before, when $\lambda \notin (-\infty, -\alpha]$, we can solve for ϕ to obtain

$$\phi(r, \theta) = -\hat{\psi}(r, \lambda)(p_1\cos\theta + p_2\sin\theta),$$

where $\hat{\psi} = F(S(r_0))\ (\mathrm{L}_R^1 + \lambda)^{-1}\delta_{r_0}$. A simple evaluation of $\displaystyle\int_{C_{r_0}} \phi d\vec{s}$ reveals that $\lambda \notin (-\infty, -\alpha]$ is an eigenvalue of $\mathbf{L}$ if and only if

$$b\lambda + S'(r_0) + \hat{\psi}(r_0, \lambda) = 0, \qquad \hat{\psi} = F(S(r_0))\,(\mathrm{L}_R^1 + \lambda)^{-1}\delta_{r_0}, \tag{21}$$

where $b = (\pi r_0 \beta \Gamma'(S(r_0)))^{-1}$ is the same as before.

Taking the inner product of $(\mathrm{L}_R^1 + \lambda)\hat{\psi} = F\delta_{r_0}$ with $\hat{\psi}$ and S', respectively, we obtain

$$F(S(r_0))\hat{\psi}(r_0, \lambda) = (L_R^1\hat{\psi}, \hat{\psi})_R + \lambda\|\hat{\psi}\|_R^2, \tag{22}$$

$$\lambda(\hat{\psi}, S')_R = 2\pi r_0 F(S(r_0))[S'(r_0) + \hat{\psi}(r_0, \lambda)]. \tag{23}$$

From the second equation, we see that λ is an eigenvalue if and only if

$$\lambda\ \{\ 2\pi r_0 b F(S(r_0)) + (S', \hat{\psi}(\cdot, \lambda))_R\ \} = 0.$$

Here, (19) and (20) imply that $(S', \psi(r_0, \lambda))_R$ is not real if λ is not real. Hence, we conclude that all eigenvalues are real, and $\lambda \in (-\alpha, 0) \cup (0, \infty)$ is an eigenvalue if and only if

$$2\pi r_0 - bF(S(r_0)) + (S', \hat{\psi}(\cdot, \lambda))_R = 0. \tag{24}$$

Note that (i) $S' < 0$, (ii) $\hat{\psi}(\cdot, \lambda) > 0$ for all $\lambda > -\alpha$, (iii) $\hat{\psi}$ is decreasing in $\lambda \in (-\alpha, \infty)$, (iv) as $\lambda \to \infty$, $\hat{\psi} \to 0$. Hence, there exists a unique solution $\hat{\lambda}(b)$ solve (20) (When $b > (S', \hat{\psi}(\cdot, -\alpha))_R$), and we simply define $\hat{\lambda}(b) = -\alpha$. Since when $\lambda = 0$, $\hat{\psi} = -S'$, we see that $\hat{\lambda}(b^*) = 0$ for $b^* = (S', S')_R/(2\pi r_0 F(S(r_0))$, which is the same b^* as in the previous subsection. Hence, $\hat{\lambda}(b) < 0$ if $b > b^*$ and $\lambda > 0$ if $b < b^*$.

In the previous section, we see that when $b = b^*$, zero is an eigenvalue of L, whereas when $b \neq b^*$, zero is not an eigenvalue. Next, we investigate what happen to $\mathbf{L}$ when $b = b^*$. Hence, we assume that $b = b^*$.

From the previous analysis, we see that if $\mathbf{L}\Phi = 0$, then we must have $\Phi = (\hat{\psi}(\cdot, 0)(p_1\cos\theta + p_2\sin\theta), P)^T = (-\nabla S \cdot P, P)^T$. Hence, the space $\mathrm{Ker}(\mathbf{L}) := \{\Phi\ |\mathbf{L}\Phi = 0\}$ is two-dimensional, which is true for all other b.

Now, we show that the union of the null space of $\mathbf{L}^k$ for all $k = 1, 2, \cdots$ is four-dimensional and is spanned by $\Phi_j = (-S_{x_j}, \mathbf{e}_j)$, $j = 1, 2$, and Φ_3 and Φ_4 which

are solutions to $\mathbf{L}\Phi_{j+2} = \Phi_j$, $j = 1, 2$, where $\mathbf{e}_1 = (1, 0)$ and $\mathbf{e}_2 = (0, 1)$. For this purpose, we introduce the inner product

$$((\phi_1, P_1)^T, (\phi_2, P_2)^T)_{L^2} = \int_{\mathbb{R}^2} \phi_1 \bar{\phi}_2 \, dx + P_1 \cdot \bar{P}_2.$$

Then, it is easy to verify $(\mathbf{L}\Phi, \Psi)_{L^2} = (\Phi, \mathbf{L}^*\Psi)_{L^2}$, where

$$\mathbf{L}^* \begin{bmatrix} \phi \\ P \end{bmatrix} := \begin{bmatrix} (D\Delta - \alpha + F'H\phi + \beta\Gamma'(S(r_0))\delta_{C_{r_0}}\mathbf{e}(\theta) \cdot P \\ \beta\Gamma'(S(r_0))\pi r_0 S'(r_0)P + F(S(r_0)) \int_{C_{r_0}} \phi \, d\vec{s} \end{bmatrix}$$

It is then easy to show, for $j = 1, 2$, that $\Phi_j^* := (S_{x_j}, -\frac{F(S(r_0))}{\beta\Gamma'(S(r_0))}\mathbf{e}_j)$ satisfies $\mathbf{L}^*\Phi_j^* = 0$. In addition, the space $\mathrm{Ker}(\mathbf{L}^*) := \{\Phi \mid \mathbf{L}^*\Phi = 0\}$ is exactly spanned by Φ_1^* and Φ_2^*. It is then easy to show that $\mathrm{Ker}(\mathbf{L}) \perp \mathrm{Ker}(\mathbf{L}^*)$ if and only if $b = b^*$. With a little more work, we can show that the algebraic multiplicity of the zero eigenvalue of $\mathbf{L}$ is just four when $b = b^*$. In addition, Φ_3 and Φ_4 can be expressed in terms of the solution ψ in (11). We omit the details but present a lemma on the eigenfunctions of $\mathbf{L}$ and $\mathbf{L}^*$ at $b = b^*$.

Lemma 3.4. *Let $\phi_0(r)$ be the solution of $\mathrm{L}_R^1\phi_0 = S'$, and let*

$$\mathbf{S}_1(y) := \begin{pmatrix} S'(r)\cos\theta \\ -\mathbf{e}_1 \end{pmatrix}, \ \mathbf{S}_2(y) := \begin{pmatrix} S'(r)\sin\theta \\ -\mathbf{e}_2 \end{pmatrix},$$

$$\Psi_1(y) := \begin{pmatrix} \phi_0(r)\cos\theta \\ 0 \end{pmatrix}, \ \Psi_2(y) := \begin{pmatrix} \phi_0(r)\sin\theta \\ 0 \end{pmatrix}$$

$$\Phi_1^*(y) := \begin{pmatrix} S'(r)\cos\theta \\ -\frac{F(S_0)}{\beta\Gamma'(S_0)}\mathbf{e}_1 \end{pmatrix}, \ \Phi_2^*(y) := \begin{pmatrix} S'(r)\sin\theta \\ -\frac{F(S_0)}{\beta\Gamma'(S_0)}\mathbf{e}_2 \end{pmatrix},$$

and

$$\Psi_1^*(y) := \begin{pmatrix} (-a_0 S'(r) + \phi_0(r))\cos\theta \\ \frac{a_0 F(S_0)}{\beta\Gamma'(S_0)}\mathbf{e}_1 \end{pmatrix}, \ \Psi_2^*(y) := \begin{pmatrix} (-a_0 S'(r) + \phi_0(r))\sin\theta \\ \frac{a_0 F(S_0)}{\beta\Gamma'(S_0)}\mathbf{e}_2 \end{pmatrix},$$

where $y = r\mathbf{e}(\theta)$, $S_0 := S(r_0)$ and $a_0 := \dfrac{\|\phi_0\|_R^2}{(S', \phi_0)_R}$. Then, $\mathbf{L}\mathbf{S}_j = 0$, $\mathbf{L}\Psi_j = -\mathbf{S}_j$ and $\mathbf{L}^*\Phi_j^* = 0$, $\mathbf{L}^*\Psi_j^* = -\Phi_j^*$ and the normalizations hold

$$(\mathbf{S}_j, \Phi_j^*)_{L^2} = (\Psi_j, \Psi_j^*)_{L^2} = 0, \ (\Psi_j, \Phi_j^*)_{L^2} = (\mathbf{S}_j, \Psi_j^*)_{L^2} = \frac{1}{2}(S', \phi_0)_R > 0.$$

$\mathbf{S}_j$ and Ψ_j are orthogonal to Φ_k^* and Ψ_k^* for $j \neq k$.

3.5. **A traveling wave solution (traveling spot).** When b cross b^*, the zero eigenvalue of $\mathbf{L}$ degenerates with the Jordan Block as per Lemma3.4. Since the parameter b is determined by (12), for simplicity, we hereinafter consider β as the bifurcation parameter, while all other parameters are fixed. Let β^* be the value corresponding to b^*, and write $\beta = \beta^* + \eta$ for $|\eta| << 1$. Then, (1) is given as

$$\begin{cases} c_t(x,t) = D\Delta c - \alpha\, c + F(c)H(r_0 - |x - P|), & x \in \Omega, \ t \in (0, \infty), \\ \dot{P}(t) = \beta^* \int_{C_{r_0}} \Gamma(c(P + x))d\vec{s} + \eta \int_{C_{r_0}} \Gamma(c(P + x))d\vec{s}, & t > 0. \end{cases} \tag{25}$$

The system (22) has stationary solutions $\mathbf{S}(x - P; P) := (S(x - P), P)^T$ for an arbitrarily given constant vector $P \in \mathbb{R}^2$ independent of η. Regarding $\mathbf{S}$ as a trivial solution, we consider the bifurcation structure in the neighborhood of $\eta = 0$ ($\beta = \beta^*$).

Let $\mathcal{M} := \{\mathbf{S}(\cdot - P; P)^T;\ P \in \mathbb{R}^2\}$ and $\mathbf{U}(y, \zeta, P) := \mathbf{S}(y; P) + \zeta_1\Psi_1(y) + \zeta_2\Psi_2(y)$ ($\zeta = (\zeta_1, \zeta_2)$). Define $E := span\{\mathbf{S}_1,\ \mathbf{S}_2,\ \Psi_1,\ \Psi_2\}$ and the orthogonal space $E^\perp := \{\mathbf{v};\ (\mathbf{v}, \Phi_j^*)_{L^2} = (\mathbf{v}, \Psi_j^*)_{L^2} = 0\ (j = 1, 2)\}$. Then, $\mathbf{u} = (u, \widehat{P})^T$ in the neighborhood of $\mathcal{M}$ is uniquely represented by $\mathbf{u} = \mathbf{U}(x - P; \zeta, P) + (v(x - P), \mathbf{q})$ for $P \in \mathbb{R}^2$ and $\mathbf{v} = (v(y), \mathbf{q})^T \in E^\perp$ by a standard manner.

By $\mathbf{u} = (c(x - P, t), P + \mathbf{q})^T$, (22) becomes

$$\begin{cases} c_t(y,t) = D\Delta c - \alpha\, c + F(c)H(r_0 - |y - \mathbf{q}|) + \dot{P} \cdot \nabla c, \\ \dfrac{d}{dt}(P + \mathbf{q}) = \beta^* \displaystyle\int_{C_{r_0}} \Gamma(c(\mathbf{q} + y))d\vec{s} + \eta \int_{C_{r_0}} \Gamma(c(\mathbf{q} + y))d\vec{s} \end{cases} \tag{26}$$

for $y = x - P \in \Omega$ and $t \in (0, \infty)$, which we write as

$$\mathbf{u}_t = \mathbf{A}_0(\mathbf{u}) + \eta\mathbf{G}_1(\mathbf{u}) + \mathbf{G}_2(c, \dot{P}), \tag{27}$$

where

$$\begin{aligned} \mathbf{u} &= \begin{pmatrix} c \\ P + \mathbf{q} \end{pmatrix}, \qquad \mathbf{G}_2(c, \dot{P}) := \begin{pmatrix} \dot{P} \cdot \nabla c \\ 0 \end{pmatrix}, \\ \mathbf{A}_0(\mathbf{u}) &:= \begin{pmatrix} D\Delta c - \alpha\, c + F(c)H(r_0 - |y - \mathbf{q}|) \\ \beta^* \int_{C_{r_0}} \Gamma(c(\mathbf{q} + y))d\vec{s} \end{pmatrix}, \\ \mathbf{G}_1(\mathbf{u}) &:= \begin{pmatrix} 0 \\ \int_{C_{r_0}} \Gamma(c(\mathbf{q} + y))d\vec{s} \end{pmatrix}. \end{aligned}$$

By the representation of $\mathbf{u} = \mathbf{U}(y; \zeta, P) + \mathbf{v}$ with $\mathbf{v} = (v(y, t), \mathbf{q}) \in E^\perp$, (24) becomes

$$\begin{aligned} \mathbf{v}_t &= \mathbf{L}\mathbf{v} + \mathbf{L}(\zeta_1\Psi_1 + \zeta_2\Psi_2) - (\dot{\zeta_1}\Psi_1 + \dot{\zeta_2}\Psi_2) + \frac{1}{2}\mathbf{A}_0''(\mathbf{S})(\zeta_1\Psi_1 + \zeta_2\Psi_2 + \mathbf{v})^2 + \cdots \\ &\quad + \eta\mathbf{G}_1(\mathbf{U} + \mathbf{v}) + \mathbf{G}_2(U, \dot{P}) - (0, \dot{P})^T + \mathbf{G}_2(\mathbf{v}, \dot{P}) \\ &= \mathbf{L}\mathbf{v} - (\zeta_1\mathbf{S}_1 + \zeta_2\mathbf{S}_2) - (\dot{\zeta_1}\Psi_1 + \dot{\zeta_2}\Psi_2) + \frac{1}{2}\mathbf{A}_0''(\mathbf{S})(\zeta_1\Psi_1 + \zeta_2\Psi_2 + \mathbf{v})^2 + \cdots \\ &\quad + \eta\mathbf{G}_1(\mathbf{U} + \mathbf{v}) + \dot{p_1}\mathbf{S}_1 + \dot{p_2}\mathbf{S}_2 + \mathbf{G}_2(\zeta_1\Psi_1 + \zeta_2\Psi_2, \dot{P}) + \mathbf{G}_2(\mathbf{v}, \dot{P}), \end{aligned}$$

where $\mathbf{L} = \mathbf{A}_0'(\mathbf{S})$ and $P = (p_1, p_2)^T$. Thus, all the necessary properties of the equation for $\mathbf{v}$ are satisfied together with the property of $\mathbf{L}$, as in Lemma 3.4, so that we can apply the results of [1]. As a consequence, we have the following results corresponding to Theorem 2.2 in [1]:

Lemma 3.5. *$P(t)$ and $\zeta(t) = (\zeta_1(t), \zeta_2(t))$ satisfy*

$$\begin{cases} \dot{P} &= \zeta + O(|\zeta|^3 + |\eta|^{\frac{3}{2}}), \\ \dot{\zeta} &= -\nabla_\zeta W + O(|\zeta|^4 + |\eta|^2) \end{cases} \tag{28}$$

as long as $|\zeta| < \zeta^*$ *and* $|\eta| < \eta^*$ *for positive constants* ζ^* *and* η^*, *where* $W = W(\zeta) := \frac{1}{4}M_1|\zeta|^4 + \frac{1}{2}M_2\eta|\zeta|^2$. M_1 *and* M_2 *are given by*

$$\begin{aligned} M_1 &:= \frac{2}{(S',\phi_0)_R}\Big(-\frac{1}{8}\{\int_0^{r_0} rF'''(S(r))\phi_0^3(r)S_r(r)dr - \frac{\Gamma'''(S_0)}{\Gamma'(S_0)}\phi_0^3(r_0)F(S_0)\} \\ &\quad -\frac{1}{4}\int_0^{r_0} rF''(S(r))\phi_0(r)(V_1(r)+\frac{1}{2}W_1(r))S_r(r)dr \\ &\quad +\frac{\Gamma''(S_0)F(S_0)\phi_0(r_0)}{4\Gamma'(S_0)}(V_1(r_0)+\frac{1}{2}W_1(r_0)) \\ &\quad -\frac{1}{2}\int_0^{r_0}(2r\partial_r V_1(r)+r\partial_r W_1(r)+2W_1(r))S_r(r)dr\Big), \\ M_2 &:= \frac{\phi_0(r_0)F(S_0)}{\beta^*(S',\phi_0)_R}, \end{aligned}$$

where $V_1(r)$ *and* $W_1(r)$ *are the solutions of*

$$-\mathrm{L}_R^0 V_1 = \frac{1}{2}\Big(\partial_r\phi_0 - \frac{1}{2}F''(S(r))H(r_0-r)\phi_0^2 + \frac{1}{r}\phi_0(r)\Big), \tag{29}$$

$$-\mathrm{L}_R^2 W_1 = \frac{1}{2}\Big(\partial_r\phi_0 - \frac{1}{2}F''(S(r))H(r_0-r)\phi_0^2 - \frac{1}{r}\phi_0(r)\Big), \tag{30}$$

respectively and $\mathrm{L}_R^N := -D\Big(\frac{d^2}{dr^2}+\frac{1}{r}\frac{d}{dr}-\frac{N^2}{r^2}\Big) - F'(S(r))H(r_0-r)+\alpha$.

Proof. The proof is basically the same as that for Theorem 2.2 in [1]. We simply show that the constants M_1 and M_2 are given by the above equations.

First, we shall consider M_1. From (25), we have

$$\dot{\zeta_1} = -M_1(\zeta_1^2+\zeta_2^2)\zeta_1 - M_2\eta\zeta_1 + h.o.t.$$

Thus, M_1 is the coefficient of ζ_1^3 and $\zeta_2^2\zeta_1$. According to the proof of Theorem 2.2 ([1]), ζ_1^3 and $\zeta_2^2\zeta_1$ are derived from

$$\frac{1}{6}(\mathbf{A}_0'''(\mathbf{S})(\zeta_1\Psi_1+\zeta_2\Psi_2)^3, \Phi_1^*)_{L^2}, \tag{31}$$

$$(\mathbf{A}_0''(\mathbf{S})(\zeta_1\Psi_1)(\zeta_1^2\mathbf{v}_1), \Phi_1^*)_{L^2}, \tag{32}$$

$$-(\partial_x\mathbf{v}_1, \Phi_1^*)_{L^2}, \tag{33}$$

where the function $\mathbf{v}_1$ is defined by

$$-\mathbf{L}\mathbf{v}_1 = \frac{1}{2}\mathbf{A}_0''(\mathbf{S})\Psi_1^2 + \partial_{y_1}\Psi_1.$$

First, we consider the coefficient ζ_1^3 in (28), that is,

$$\frac{1}{6}(\mathbf{A}_0'''(\mathbf{S})\Psi_1^3, \Phi_1^*)_{L^2}.$$

We calculate

$$\begin{aligned} &(\mathbf{A}_0'''(\mathbf{S})\Psi_1^3, \Phi_1^*)_{L^2} \\ &= \Big(\begin{pmatrix} \cos^3\theta F'''(S(r))H(r_0-r)\phi_0^3(r) \\ \beta^*\Gamma'''(S_0)\displaystyle\int_{C_{r_0}}\cos^3\theta\phi_0(r)\,d\vec{s} \end{pmatrix}, \begin{pmatrix} S_r\cos\theta \\ -\dfrac{F(S_0)}{\beta^*\Gamma'(S_0)}\mathbf{e}_1 \end{pmatrix}\Big)_{L^2} \\ &= \frac{3}{4}\pi M_1', \end{aligned}$$

where

$$M_1' := \int_0^{r_0} rF'''(S(r))\phi_0^3(r)S'(r)dr - \frac{\Gamma'''(S_0)}{\Gamma'(S_0)}\phi_0^3(r_0)F(S_0).$$

Next, consider (29), that is,

$$(\mathbf{A}_0''(\mathbf{S})\Psi_1 \cdot \mathbf{v}_1, \Phi_1^*)_{L^2}. \tag{34}$$

This requires the calculation of $\mathbf{v}_1$. Since the equation of $\mathbf{v}_1$ is written for $\mathbf{v}_1 = (v, \mathbf{q})$

$$\begin{aligned}
\mathbf{L}\mathbf{v}_1 &= \begin{pmatrix} (D\Delta - \alpha + F'(S(r))H(r_0 - r)v + F(S_0)\delta(r_0 - r)\mathbf{e}(\theta)\cdot\mathbf{q} \\ \beta^*\Gamma'(S_0)[\pi r_0 S'\mathbf{q} + \int_{C_{r_0}} v d\vec{s}] \end{pmatrix} \\
&= \begin{pmatrix} (\cos^2\theta\partial_r\phi_0 - \frac{\sin^2\theta}{r}\phi_0) + \frac{1}{2}F''(S(r))H(r_0 - r)\cos^2\theta\phi_0^2(r) \\ \frac{1}{2}\beta^* F''(S_0)\int_{C_{r_0}} \cos^2\theta\phi_0^2(r)d\vec{s} \end{pmatrix} \\
&= \begin{pmatrix} (\cos^2\theta\partial_r\phi_0 + \frac{\sin^2\theta}{r}\phi_0) - \frac{1}{2}F''(S(r))H(r_0 - r)\cos^2\theta\phi_0^2(r) \\ 0 \end{pmatrix},
\end{aligned}$$

$\mathbf{v}_1 = \begin{pmatrix} V_1(r) + \cos 2\theta W_1(r) \\ 0 \end{pmatrix}$ satisfies the above equation of $\mathbf{v}_1$ together with $\mathbf{v}_1 \in E^\perp$ if V_1 and W_1 are defined by (26) and (27). Substituting $\mathbf{v}_1$ of this form into (31), we have

$$(\mathbf{A}_0''(\mathbf{S})\Psi_1 \cdot \mathbf{v}_1, \Phi_1^*)_{L^2} = \pi M_1'',$$

where

$$\begin{aligned}
M_1'' &:= \int_0^{r_0} rF''(S(r))\phi_0(r)(V_1(r) + \frac{1}{2}W_1(r))S'(r)dr \\
&\quad - \frac{\Gamma''(S_0)F(S_0)\phi_0(r_0)}{4\Gamma'(S_0)}(V_1(r_0) + \frac{1}{2}W_1(r_0)).
\end{aligned}$$

Finally, we obtain (30). Since

$$\partial_x\mathbf{v}_1 = \cos\theta\partial_r\mathbf{v}_1 + \frac{\sin\theta}{r}\partial_\theta\mathbf{v}_1 = \begin{pmatrix} \cos\theta\partial_r V_1 + \cos\theta\cos 2\theta\partial_r W_1 - \frac{2\sin\theta\sin 2\theta}{r}W_1 \\ 0 \end{pmatrix},$$

(30) is calculated as

$$\pi M_1''' := -(\partial_x\mathbf{v}_1, \Phi_1^*)_{L^2} = -\frac{1}{2}\pi\int_0^{r_0}(2r\partial_r V_1(r) + r\partial_r W_1(r) + 2W_1(r))S_r(r)dr.$$

Thus, the coefficient of ζ_1^3 is given by $\frac{1}{6}\cdot\frac{3}{4}\pi M_1' + \pi M_1'' + \pi M_1''' = \pi(\frac{1}{8}M_1' + M_1'' + M_1''')$. Since $(\Psi_1, \Phi_1^*)_{L^2} = \frac{1}{2}\pi(S', \phi_0)_R$ from Lemma3.4, M_1 is given by $M_1 = -\frac{2}{(S', \phi_0)_R}(\frac{1}{8}M_1' + M_1'' + M_1''')$, which is used in this lemma.

Similarly, M_2 is given by

$$M_2 = -\frac{2}{(S', \phi_0)_R}(\mathbf{G}_1'(\mathbf{S})\Psi_1, \Phi_1^*)_{L^2},$$

which proves this lemma. □

Remark 2. By Lemma 3.5, ζ denotes the deformation of solution c from the radially symmetric solution $S(y)$ as well as the velocity of the camphor disc, because ζ gives $\dot{P}$ for the location $P(t)$.

Remark 3. Here, $\phi_0(r) \leq 0$, and $F(c)$ is positive. Hence, M_2 is a negative constant, while the sign of M_1 is not fixed and depends on various factors, such as F, Γ, and. in particular, the radius of the camphor disc, r_0.

Remark 4. The negative sign of the constant M_2 and (25) implies that the radially symmetric stationary solution $\mathbf{S}(x-P;P)$ is stable for $\eta < 0 (\beta < \beta^*)$ and unstable for $\eta > 0 (\beta > \beta^*)$, whereas the sign of M_1 determines the direction of bifurcation, that is, super-critical bifurcation occurs when $M_1 > 0$ and sub-critical bifurcation occurs when $M_1 < 0$.

4. **Interaction of spots.** In the introduction, we observed that a moving disc is reflected by a wall, as shown in Figure 1. In order to clarify this property, two moving spots are located in a mirror symmetric manner such that they reflect each other when they approach each other closely. For this purpose, we consider the interaction of the two moving spots. Assume Ω to be $\mathbb{R}^2$. The model equation of multiple camphor discs is

$$\begin{cases} c_t = D\Delta c - \alpha\, c + F(c) \sum_{j=1}^m H(r_j - |x - P_j|), & x \in \mathbb{R}^2,\ t \in (0,\infty), \\ \dot{P}_j(t) = \beta_j \int_{C_{r_j}} \Gamma(c(P_j + x) d\vec{s}, & t > 0,\ j = 1, \cdots, m. \end{cases} \tag{35}$$

For simplicity, we consider only the case of two discs ($m = 2$). Let $\mathbf{S}_1(y;P_1) := (S_1(y), P_1, 0)^T$ and $\mathbf{S}_2(y;P_2) := (S_2(y), 0, P_2)^T$, where $S_j(y)$ are the radially symmetric solutions with radius $r = r_j$ $(j = 1, 2)$ discussed in Section 3.1. We assume the asymptotic forms as

$$S_j(r) \to \frac{1}{\sqrt{r}} e^{-\alpha r} b_j \ (r \to \infty).$$

We write (32) ($m = 2$) by $y = x - P_1$ and $\mathbf{h} = P_2 - P_1$

$$\begin{cases} c_t &= D\Delta c - \alpha\, c + F(c)\{H(r_1 - r) + H(r_2 - |y - \mathbf{h}|)\} + \dot{P}_1 \cdot \nabla c, \\ \dot{P}_1(t) &= \beta_1 \int_{C_{r_1}} \Gamma(c(y)) d\vec{s}, \\ \dot{P}_2(t) &= \beta_2 \int_{C_{r_2}} \Gamma(c(y - \mathbf{h})) d\vec{s}, \end{cases} \tag{36}$$

or simply

$$\mathbf{u}_t = \mathbf{A}(\mathbf{u}) + (\dot{P}_1 \cdot \nabla c, 0, 0)^T$$

for $\mathbf{u} = (c, P_1, P_2)^T$. Here, we assume that β_1 is close to the bifurcation point, say β_1^*, as in the previous section, whereas this assumption is not made for β_2. Let $\beta_1 = \beta_1^* + \eta$. We write $\mathbf{A} = \mathbf{A}_0 + \eta \mathbf{G}$.

We consider only the dynamics of P_1 and ζ_1, and in the remainder of this section, we simply express S_1, β_1, and r_1 as S, β, and r_0. The dynamics of $P = P_1 = (p_1, p_2)^T$ and $\zeta = \zeta_1 = (\zeta_1, \zeta_2)^T$ are then basically given by

$$\begin{cases} \dot{P} &= \zeta + \dfrac{2}{(S', \phi_0)_{L^2}} \begin{pmatrix} (\mathbf{A}_0(\mathbf{S}(y;P) + \mathbf{S}_2(y - \mathbf{h}; P_2)), \Psi_1^*)_{L^2} \\ (\mathbf{A}_0(\mathbf{S}(y;P) + \mathbf{S}_2(y - \mathbf{h}; P_2)), \Psi_2^*)_{L^2} \end{pmatrix} + h.o.t. \\ \dot{\zeta} &= -\nabla_\zeta W + \dfrac{2}{(S', \phi_0)_{L^2}} \begin{pmatrix} (\mathbf{A}_0(\mathbf{S}(y;P) + \mathbf{S}_2(y - \mathbf{h}; P_2)), \Phi_1^*)_{L^2} \\ (\mathbf{A}_0(\mathbf{S}(y;P) + \mathbf{S}_2(y - \mathbf{h}; P_2)), \Phi_2^*)_{L^2} \end{pmatrix} + h.o.t. \end{cases} \tag{37}$$

which are obtained in a manner similar to the system in Theorem 4.1 [1]. Here, Ψ_1^* denotes $\Psi_1^* = (-a_0S'(r) + \phi_0(r))\cos\theta, \frac{a_0F(S_0)}{\beta\Gamma'(S_0)}\mathbf{e}_1, 0)^T$, and the remaining notation is similar to that used in Theorem 4.1.

Lemma 4.1. *Let* $h := |\mathbf{h}|$, $\mathbf{e} = (e_1, e_2)^T := \dfrac{1}{h}(P_2 - P)$. *Then*

$$(\mathbf{A}_0(\mathbf{S}(y;P) + \mathbf{S}_2(y-\mathbf{h};P_2)), \Psi_j^*)_{L^2} = \frac{b_2}{\sqrt{h}}e^{-\alpha h}M_0e_j(1+o(1)) \ (j=1,2),$$

$$(\mathbf{A}_0(\mathbf{S}(y;P) + \mathbf{S}_2(y-\mathbf{h};P_2)), \Phi_j^*)_{L^2} = \frac{b_2}{\sqrt{h}}e^{-\alpha h}\overline{M_0}e_j(1+o(1)) \ (j=1,2),$$

hold, where

$$M_0 := a_0F(S_0)r_0\int_0^{2\pi} e^{\alpha r_0\cos\theta}\cos\theta d\theta + \int_0^{r_0} G_0(r)\int_0^{2\pi} e^{\alpha r\cos\theta}\cos\theta d\theta dr$$

with $G_0(r) := \{F'(S(r)) - F'(0)\}(-a_0S'(r) + \phi_0(r))$, *and*

$$\overline{M_0} := a_0F(S_0)r_0\int_0^{2\pi} e^{\alpha r_0\cos\theta}\cos\theta d\theta + \int_0^{r_0} G_1(r)\int_0^{2\pi} e^{\alpha r\cos\theta}\cos\theta d\theta dr$$

with $G_1(r) := \{F'(S(r)) - F'(0)\}S'(r)$,

Proof. Since the proof of this lemma is quite similar to the proof of Theorem 4.2 [1], we present only an outline by showing the first equation of this lemma

$$(\mathbf{A}_0(\mathbf{S}(y;P) + \mathbf{S}_2(y-\mathbf{h};P_2)), \Psi_j^*)_{L^2} = \frac{b_2}{\sqrt{h}}e^{-\alpha h}M_0e_1(1+o(1)),$$

but the other equations are omitted.

Let $\mathbf{A}_0 = (\mathcal{L}_1(c), \mathcal{L}_2(c), \mathcal{L}_3(c))^T$. Then. the left-hand side of the above expression is

$$(\mathcal{L}_1(S(y)+S_2(y-\mathbf{h})), (-a_0S'+\phi_0)\cos\theta)_{L^2} + \frac{a_0F(S_0)}{\Gamma'(S_0)}\int_{C_{r_0}}\Gamma(S(y)+S_2(y-\mathbf{h}))\cos\theta ds,$$

where $y = r_0(\cos\theta, \sin\theta)^T$.

First, we calculate

$$\frac{a_0F(S_0)}{\Gamma'(S_0)}\int_{C_{r_0}}\Gamma(S(y) + S_2(y-\mathbf{h}))\cos\theta ds. \tag{38}$$

Since $S_2(y-\mathbf{h}) \sim \dfrac{1}{\sqrt{|y-\mathbf{h}|}}e^{-\alpha|y-\mathbf{h}|}b_2 \sim \dfrac{1}{\sqrt{h}}e^{-\alpha h}e^{-\alpha r\cos(\theta-\gamma)}b_2$ for $e_1 = \cos\gamma$, we substitute this expression into (35) to obtain

$$\begin{aligned}
&\frac{a_0F(S_0)}{\Gamma'(S_0)}\left(\int_{C_{r_0}}\Gamma(S(y))\cos\theta ds + \int_{C_{r_0}}\Gamma'(S(y))S_2(y-\mathbf{h})\cos\theta ds\right)\\
&\quad\sim\quad a_0F(S_0)\int_{C_{r_0}} S_2(y-\mathbf{h})\cos\theta ds\\
&\quad\sim\quad a_0F(S_0)\frac{1}{\sqrt{h}}e^{-\alpha h}b_2r_0e_1\int_0^{2\pi} e^{\alpha r_0\cos\theta}\cos\theta d\theta.
\end{aligned}$$

Here, $f \sim g$ denotes $f = (1 + o(1))g$ as $h \to \infty$. Thus,

$$\frac{a_0 F(S_0)}{\Gamma'(S_0)} \int_{C_{r_0}} \Gamma(S(y) + S_2(y - \mathbf{h})) \cos\theta ds \sim \frac{b_2}{\sqrt{h}} e^{-\alpha h} a_0 F(S_0) r_0 e_1 \int_0^{2\pi} e^{\alpha r_0 \cos\theta} \cos\theta d\theta \tag{39}$$

holds.

Next, we compute

$$(\mathcal{L}_1(S(y) + S_2(y - \mathbf{h})), (-a_0 S' + \phi_0)\cos\theta)_{L^2}.$$

Since

$$\begin{aligned} &\mathcal{L}_1(S(y) + S_2(y - \mathbf{h})) \\ &\quad \sim \quad \{F'(S(r)) - F'(0)\}\{H(r_0 - r) + H(r_2 - |y - \mathbf{h}|)\} \frac{1}{\sqrt{h}} e^{-\alpha h} e^{\alpha r \cos(\theta - \gamma)} b_2, \end{aligned}$$

we see that

$$\begin{aligned} &(\mathcal{L}_1(S(y) + S_2(y - \mathbf{h})), (-a_0 S' + \phi_0)\cos\theta)_{L^2} \\ \sim &\frac{b_2}{\sqrt{h}} e^{-\alpha h} \int_0^{r_0} r\{F'(S(r)) - F'(0)\}(-a_0 S'(r) + \phi_0(r)) \int_0^{2\pi} e^{\alpha r \cos\theta} \cos(\theta + \gamma) d\theta dr \\ = &\frac{b_2}{\sqrt{h}} e^{-\alpha h} e_1 \int_0^{r_0} G_0(r) \int_0^{2\pi} e^{\alpha r \cos\theta} \cos\theta d\theta dr, \end{aligned}$$

where $G_0(r) := r\{F'(S(r)) - F'(0)\}(-a_0 S'(r) + \phi_0(r))$. Thus, based on the above considerations, and taking (36) into account, this lemma is proven. □

Remark 5. For a simple example of F such as $F(c) = F_0 - d_0 c$ for positive constants F_0 and d_0, $G_0(r) = G_1(r) = 0$ holds, and the coefficients M_0, $\overline{M_0}$ can be simply calculated to be positive.

If two camphor discs are identical, that is, $r_1 = r_2 =: r_0$ and $\beta_2 = \beta_1 =: \beta^* + \eta$ in (32), then by (34) and Lemma4.1, the movement of two interacting discs is essentially described as follows:

$$\begin{cases} \dot{P}_1 &= \zeta_1 - \dfrac{M_0^*}{\sqrt{h}} e^{-\alpha h} \mathbf{e}, \\ \dot{\zeta}_1 &= -\nabla_\zeta W - \dfrac{\overline{M_0^*}}{\sqrt{h}} e^{-\alpha h} \mathbf{e}, \\ \dot{P}_2 &= \zeta_2 + \dfrac{M_0^*}{\sqrt{h}} e^{-\alpha h} \mathbf{e}, \\ \dot{\zeta}_2 &= -\nabla_\zeta W + \dfrac{\overline{M_0^*}}{\sqrt{h}} e^{-\alpha h} \mathbf{e}, \end{cases} \tag{40}$$

where $\mathbf{e} := (e_1, e_2)^T := \dfrac{1}{h}(P_2 - P_1)$, $M_0^* := -\dfrac{2}{(S', \phi_0)_{L^2}} b_0 M_0$, $\overline{M_0^*} := -\dfrac{2}{(S', \phi_0)_{L^2}} b_0 \overline{M_0}$, and $b_0 := b_1 = b_2$.

Moreover, if two discs are mirror-symmetric with respect to the y-axis in $\mathbb{R}^2$, then for $P_2 = (p, q)^T$ and $\zeta_2 = (\zeta, \xi)^T$, P_1 and ζ_1 are, respectively, given by $P_1 = (-p, q)^T$

and $\zeta_1 = (-\zeta, \xi)^T$, which makes (37) simpler as

$$\begin{cases} \dot{p} &= \zeta + \dfrac{M_0^*}{\sqrt{2p}} e^{-2\alpha p}, \\ \dot{q} &= \xi, \\ \dot{\zeta} &= -\{M_1(\zeta^2+\xi^2) + M_2\eta\}\zeta + \dfrac{\overline{M_0^*}}{\sqrt{2p}} e^{-2\alpha p}, \\ \dot{\xi} &= -\{M_1(\zeta^2+\xi^2) + M_2\eta\}\xi. \end{cases} \tag{41}$$

Figure 3 shows a numerical simulation of (38). Thus, the reflection behavior observed in the experiment (Figure1) is theoretically confirmed by the reduced equation (38).

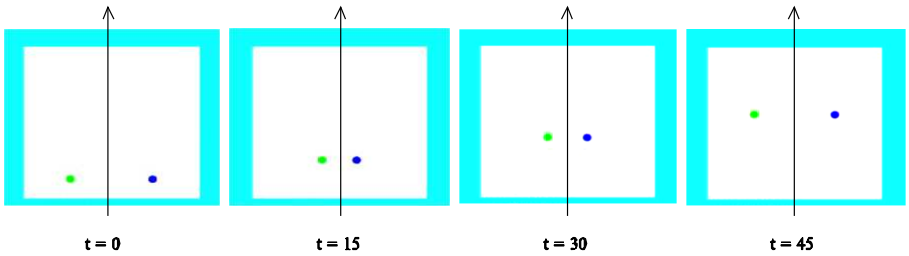

FIGURE 3. Interaction of two moving spots of (38), which are mirror symmetric in $\mathbb{R}^2$. Numerical simulation of (38) with $\eta = 0.06$, $M_1 = -M_2 = M_0^* = \overline{M_0^*} = 1$.

5. **Concluding remarks.** Several types of model equations describing camphor movements have been proposed (e.g., see [1], [5]). If a camphor scrap is disc shaped, numerical simulations show that such model equations have similar bifurcation diagrams with respect to certain parameters, which is a pitchfork bifurcation of traveling spots. It is shown that the model equation in the present paper also has a similar pitchfork bifurcation diagram. We emphasize here that the bifurcation diagram is shown theoretically together with eigenfunctions. The equation describing the motion of two interacting spots is also derived theoretically. This reveals that the interaction is repulsive. Therefore, the model equation introduced in the present paper is important and will be useful in the precise analysis of camphor motions.

As an application of the reduced ODE (37), we considered the problem of a moving camphor disc in a rectangular domain. This problem is presented as a new type of billiard problem ([4]). In [4], it was reported that a camphor disc follows a complicated orbit in the domain, which is quite different from the usual orbits in billiard problems.

REFERENCES

[1] S.-I. Ei, M. Mimura and M. Nagayama, *Interacting spots in reaction diffusion systems*, DCDS **14** (2006), 31–62.

[2] S.-I. Ei, M. Mimura and M. Nagayama, *Dynamics of spot solutions in reaction-diffusion systems in rectangular domains*, in preparation.

[3] Y. Hayashima, M. Nagayama and S. Nakata, *A camphor grain oscillates while breaking symmetry*, J. Phys. Chem. B, **105** (2001), 5353–5357.

[4] M. Mimura, T. Miyaji and I. Ohnishi, *A billiard problem in nonlinear and nonequilibrium systems*, Hiroshima Math. J., **37** (2007), 343–384

[5] M. Nagayama, S. Nakata, Y. Doi and Y. Hayashima, *A theoretical and experimental study on the unidirectional motion of a camphor disk*, Physica D, **194** (2004), 151–165.

Received July 2008; revised October 2008.

E-mail address: xinfu@pitt.edu
E-mail address: ichiro@math.kyushu-u.ac.jp
E-mail address: mimura@math.meiji.ac.jp